Multi-scale fatigue damage analysis in filament-wound carbon fiber reinforced epoxy composites for hydrogen storage tanks

Imen Feki, Mohammadali Shirinbayan, Samia Nouira, Robert Tie Bi, Jean-Baptiste Maeso, Cedric Thomas, Joseph Fitoussi

Composites Part C: Open Access 15 (2024) 100537

Contents lists available at ScienceDirect

Composites Part C: Open Access

journal homepage: www.sciencedirect.com/journal/composites-part-c-open-access

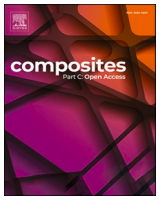

Multi-scale fatigue damage analysis in filament-wound carbon fiber reinforced epoxy composites for hydrogen storage tanks

Imen Feki [a], Mohammadali Shirinbayan [a,*], Samia Nouira [a], Robert Tie Bi [b], Jean-Baptiste Maeso [b], Cedric Thomas [b], Joseph Fitoussi [a]

[a] Arts et Metiers Institute of Technology, CNAM, CNRS, PIMM, HESAM University, F-75013, Paris, France
[b] Faurecia Hydrogen Solutions, FORVIA Clean Mobility, Bois Sur Prés, 25550, Bavans, France

ARTICLE INFO

Keywords:
Hydrogen
CFRP
Porosity
Fatigue
Damage

ABSTRACT

This article presents the findings of a multi-scale experimental study on carbon fiber-reinforced epoxy composites (CFRP) used in lightweight hydrogen storage pressure vessels produced via filament winding. The research employs a combination of tension-tension load-controlled fatigue tests and high-resolution physical-chemical characterization and porosity quantification to assess the impact of porosity on mechanical performance. The findings demonstrate that porosity has a detrimental impact on mechanical properties, acting as nucleation sites for damage mechanisms such as crack initiation, fiber-matrix separation and fiber breakage. At the mesoscopic level, microdefects coalesce into transverse cracks and delamination, resulting in complex failure modes under cyclic loading. The results of the tensile tests demonstrated that the orientation of the fibers has a significant impact on the mechanical behavior of the material. The ±15° configuration demonstrated superior tensile strength and modulus, while the ±30° and multilayer configurations exhibited higher ductility. The results of the fatigue testing confirmed that fiber orientation has a significant impact on fatigue life, with the ±15° configuration proving to be the most resistant. Microscopic analysis indicated that pores act as damage initiation points, accelerating failure through matrix cracking, fiber-matrix debonding, and delamination. This study highlights the need for improved porosity control during manufacturing to enhance the durability of hydrogen storage systems. Additionally, it provides valuable insights for optimizing fiber orientation to improve fatigue performance in practical applications.

1. Introduction

Over the past three decades, the environment has been affected by the combined effects of the depletion of fossil resources (oil, natural gas, and coal) and global warming due to the significant increase in carbon dioxide (CO_2) concentration, which is a greenhouse gas. In order to compensate for the emissions generated by conventional energy systems, it is essential to employ green energy sources that have a minimal carbon footprint. In this context, hydrogen represents a promising candidate for meeting society's demand for sustainable development. This is not only due to its status as an especially promising energy carrier, but also because it is inexhaustible, non-polluting, and can be produced from water [1–3].

The hydrogen sector comprises a number of key stages, including production, distribution, storage and utilization. The storage of this energy carrier represents a significant technological and scientific challenge in the present day. Three main strategies for hydrogen storage have been identified: solid storage (hydrogen atoms stored as simple or complex hydrides, such as borohydrides, alanates, or Li amides in a metallic crystalline network or carbon nanostructures) [4]; liquid or cryogenic storage (hydrogen volume maintained at a temperature of -250 °C) [5]; and gaseous storage (compressed storage of the maximum amount of hydrogen in a given volume). Of the aforementioned solutions, compressed gaseous storage appears to be the most developed, offering the optimal compromise in terms of mass density (ratio of stored hydrogen mass to total mass) and volumetric density (ratio of stored hydrogen volume to total volume) [6,7].

Significant advances have been made in the field of storage methods and pressures. In the case of cylinders distributed across the industry, there has been a notable increase from 200 to 350 bars. Presently,

* Corresponding author.
E-mail addresses: Imen.Feki@ensam.eu (I. Feki), Mohammadali.Shirinbayan@ensam.eu (M. Shirinbayan), Samia.Nouira@ensam.eu (S. Nouira), Robert.tbr.tiebi@forvia.com (R.T. Bi), Jean-Baptiste.Maeso@forvia.com (J.-B. Maeso), Cedric.Thomas@forvia.com (C. Thomas), Joseph.Fitoussi@ensam.eu (J. Fitoussi).

https://doi.org/10.1016/j.jcomc.2024.100537

Available online 9 November 2024

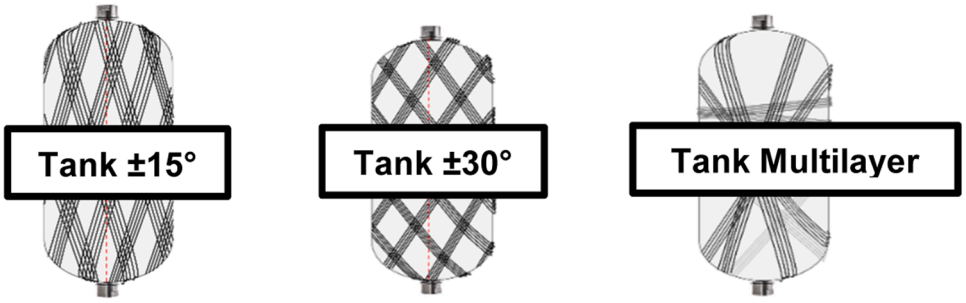

Fig. 1. Illustration of composite of cylindrical carbon fiber reinforced epoxy resin.

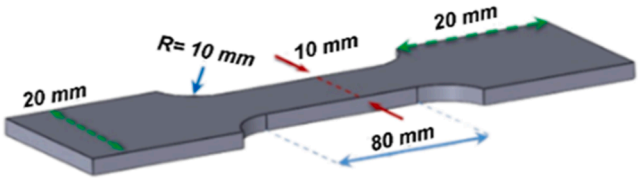

Fig. 2. Dimensions of carbon fiber reinforced epoxy samples.

research is concentrating on the creation of tanks that can withstand pressures of up to 700 bars. In this context, Type IV tanks comprise a polymer liner that ensures tightness, two metallic end fittings for the introduction and distribution of hydrogen, and a composite deposited around the liner by filament winding to ensure mechanical strength while minimizing the total mass. However, the complex environment and thermomechanical stresses experienced by the structure make it challenging to analyze the damage and failure of the composite, and consequently, to establish predictive models that enable the control of hydrogen tank design. Consequently, the prediction of burst pressure, damage state, and fatigue life in relation to filling and emptying cycles represents a significant and imperative challenge, particularly in terms

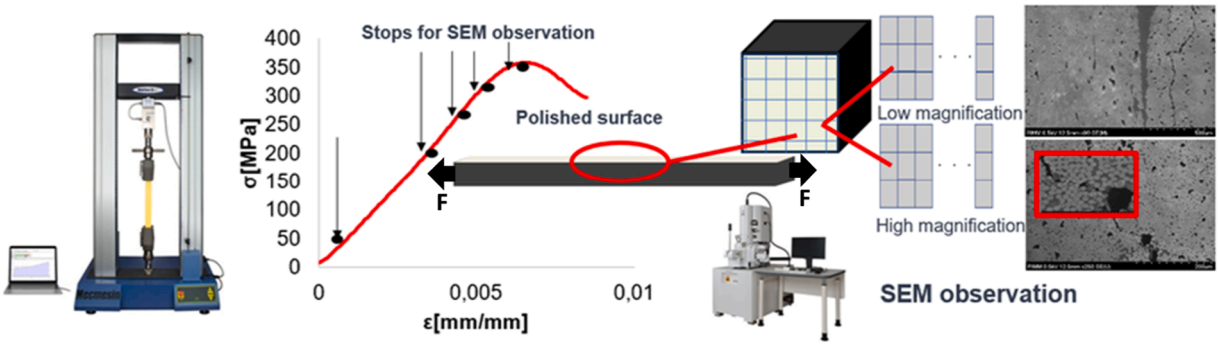

Fig. 3. Methodology used to demonstrate the specific damage phenomena.

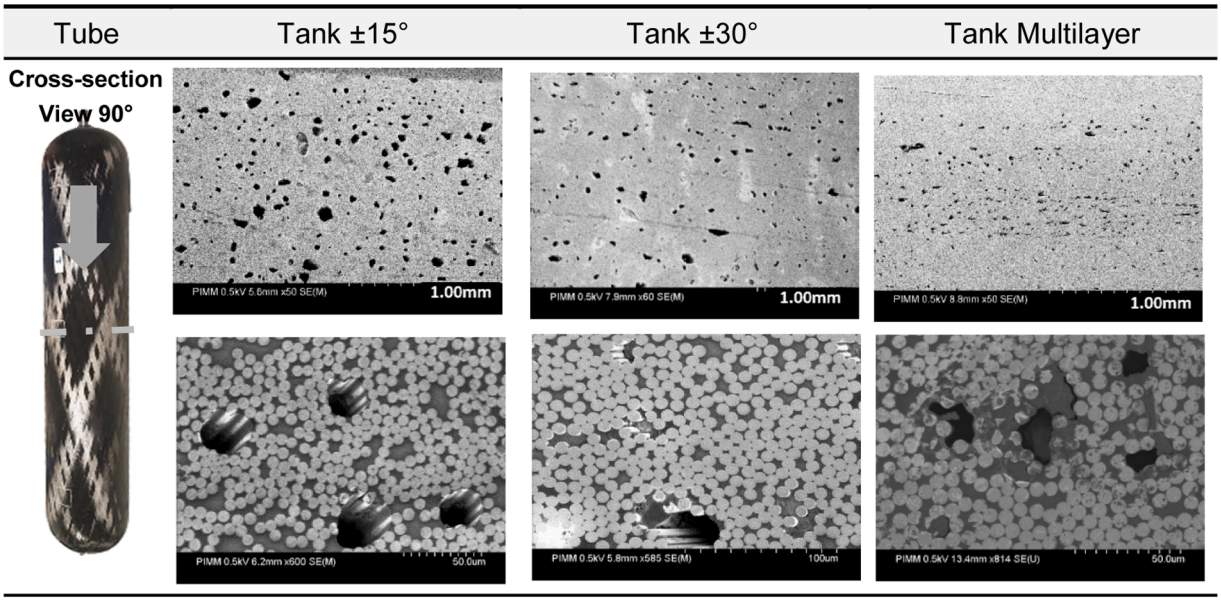

Fig. 4. SEM micrograph of carbon fiber reinforced epoxy resin samples at different orientation.

Table 1
Volume percentage of porosity in tubes with different fiber orientations.

Tube	Composite Density	Fiber (mass)	Fiber (vol)	Epoxy (mass)	Epoxy (vol)	% Volume Porosity
±15°	1,39	69,79 %	54,20 %	30,21 %	37,99 %	7,8 %
±30°	1,45	70,94 %	57,28 %	29,06 %	38,00 %	4,7 %
Multilayer	1,46	72,92 %	59,17 %	27,08 %	35,65 %	5,2 %
Average	1,44	71,15 %	56,99 %	28,85 %	37,49 %	5,4 %

Table 2
Glass transition temperature of epoxy matrix obtained from DSC.

Orientation	T_g	Observations
Tank ±15° Tank ±30° Tank Multilayer	~124 °C	Effective cross-linking, no additional peaks, no physical aging observed

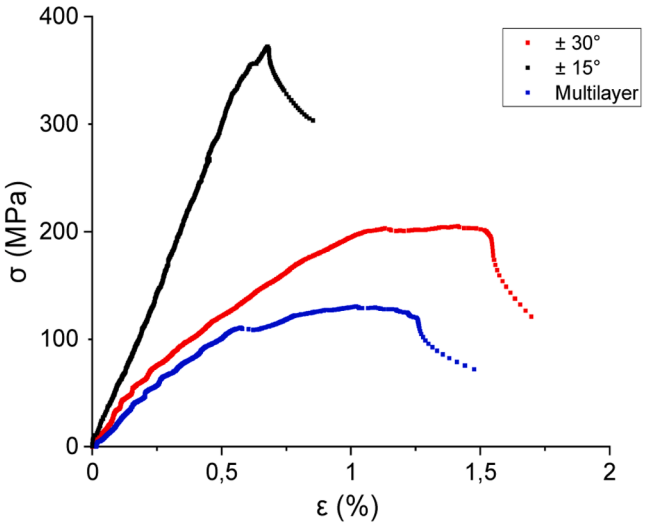

Fig. 5. Representative-curves of quasi-static tensile tests.

Table 3
Summary of tensile mechanical properties for different tubes.

Tube	E (GPa)	$\sigma_{threshold}$ (MPa)	$\varepsilon_{threshold}$ (%)	σ_{max} (MPa)	ε_{max} (%)
Tube ± 15°	$60^{\pm 2.7}$	$331^{\pm 5.2}$	$0.56^{\pm 0.02}$	$361.4^{\pm 8}$	$0.66^{\pm 0,08}$
Tube ± 30°	$36.8^{\pm 2.20}$	$55^{\pm 2.3}$	$0.17^{\pm 0.06}$	$206.6^{\pm 4.2}$	$1.3^{\pm 0,10}$
Tube Mixte	$21.1^{\pm 0.75}$	$111.8^{\pm 3.4}$	$0.538^{\pm 0.10}$	$157.1^{\pm 6.4}$	$0.94^{\pm 0,08}$

of safety [8].

Carbon fiber-reinforced polymer (CFRP) composite pressure vessels represent an efficient solution for the storage and transportation of hydrogen. In fuel cell vehicles, the fatigue lifetime of these CFRP hydrogen storage vessels represents a crucial design factor, as it directly impacts the vehicle's overall durability and reliability. However, in practice, the rapid filling of high-pressure hydrogen can result in a significant temperature increase within the vessels due to the heat released during compression and Joule-Thomson heating of the fuel [9,10]. This situation subjects the composite vessels to cyclic loading involving both high pressure and extreme temperatures, which contributes to intricate failure mechanisms such as fiber breakage, matrix cracking, and fiber/matrix interface debonding [11–13]. Over the course of the vessel's operational lifetime, numerous charging and discharging cycles are repeated, resulting in a complex thermo-mechanical fatigue failure process.

It is therefore of the utmost importance to develop reliable failure theories and fatigue life prediction methodologies that can accurately and effectively forecast the fatigue life of the composite vessel structure. A substantial body of research has demonstrated that the fatigue resistance of carbon fiber-reinforced polymer (CFRP) is significantly influenced by a multitude of intrinsic factors inherent to the composite system itself, including the types of fibers and matrix resins, the lay-up sequence, residual stresses, and defects at the fiber/matrix interface [14–16]. Each of these factors exerts a considerable influence on the fatigue damage process, including the initiation and propagation of cracks, which in turn affects the final fatigue life and failure mode. The principle forms of fatigue damage include fiber breakage, resin matrix cracking, fiber/resin debonding, and delamination. The presence of high stiffness reinforcing fibers can serve to mitigate the occurrence of matrix cracking. This is attributed to the ability of high-stiffness and strength fibers to withstand higher loads, thus limiting the strain experienced by CFRP and reducing matrix resin cracking. Thermoplastic-based composites [17–19] exhibit a reduced incidence of cracks in the matrix resin compared to thermoset-based composites [20–23]. This difference can be attributed to the high fracture toughness of thermoplastic matrix resins, which decreases the initiation and propagation of cracks at defects and stress concentration zones [24].

The phenomenon of interface debonding may occur when the bond between the fiber and matrix is found to be weak. In composites composed of multiple layers, the ply-delamination failure mode may manifest. Moreover, the fatigue resistance of CFRP is markedly affected by cyclic loads and service environments, which modify the performance of the matrix resin and the fiber/matrix interface. Consequently, fatigue is a complex phenomenon, as the lifetime of composites subjected to cyclic loading is influenced by these factors simultaneously [24].

The term "fatigue" is defined as the gradual deterioration of a material when subjected to repeated cyclic loading [25–27]. The fatigue failure mechanism of CFRP is complex due to the heterogeneous nature of the material [24]. Even when a material is subjected to load below its elastic limit, damage occurs under conditions of continuous cyclic loading. The process of material failure can be delineated into three distinct stages: the initiation of cracks, the propagation of micro-cracks, and the growth of macro-cracks. The accumulation of micro-damage progresses in a steady manner throughout the material, reaching the macro-scale where it results in macro-scale damage and material failure. Moreover, there are significant differences between low-cycle fatigue and high-cycle fatigue in terms of fatigue damage. It should be noted that low-cycle fatigue, which is characterized by high loading levels, results in irreparable damage to CFRP. Conversely, in high-cycle fatigue, the loading levels are sufficiently low for the material to remain within its elastic limit, resulting in progressive fatigue damage to composites. If the loading levels are sufficiently low, it can be assumed that no fatigue damage occurs within CFRP, resulting in an infinite fatigue life [24].

The objective of this study is to conduct an experimental investigation into the influence of fiber orientation and the effect of cyclic loading amplitude on the fatigue behavior of carbon fiber-reinforced epoxy resin composites, manufactured via the filament winding process by Faurecia Hydrogen Solutions. The study is focused on multiscale damage analysis and its impact on the overall behavior of the material under fatigue loading.

Samples of rectangular shape, with different angular orientations of the fibers, were prepared for physical, damage and mechanical characterization. These included antisymmetric laminates with angles of ±15°,

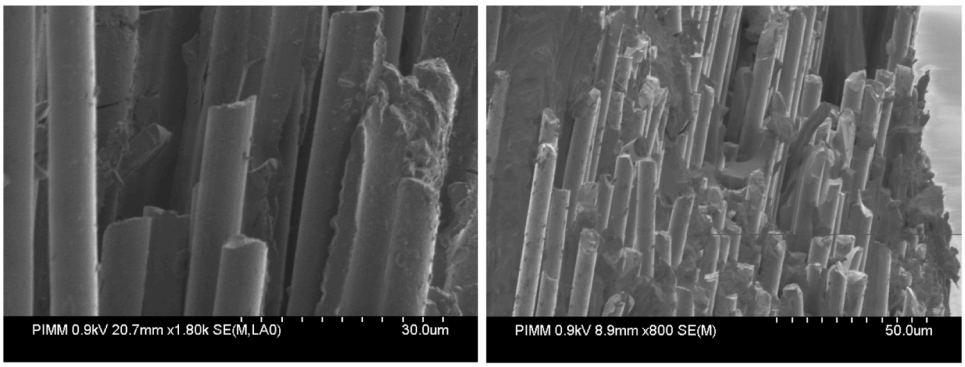

Fig. 6. Fractured surfaces of the samples after the quasi-static tensile test ±15°.

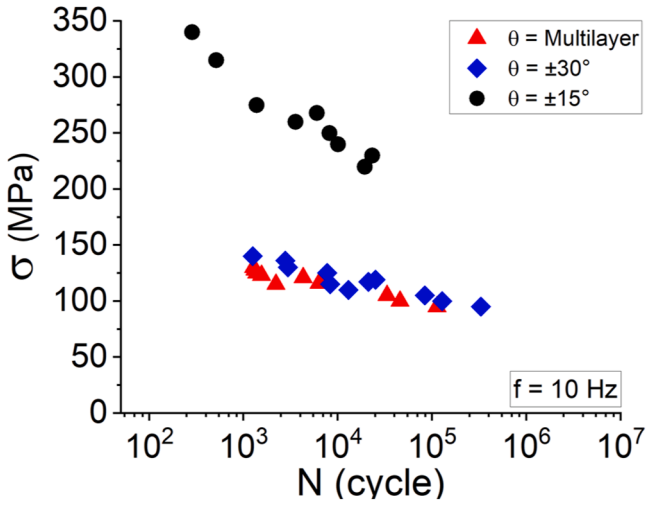

Fig. 7. Wöhler curves for samples loaded at 10 Hz.

±30°, and a multilayer combination of ±15°/±30°/±45°/±86° The article is structured as follows. The material description and methods section provides an overview of the main physical characteristics and thermal properties of the carbon fiber-reinforced epoxy composite, which were assessed using differential scanning calorimetry (DSC) and dynamic mechanical analysis (DMA) tests. Tension-tension load-controlled fatigue tests were conducted at varying maximum loadings. The results of these tests, along with a discussion of the findings, are presented in the section on experimental results and discussion. This section also includes a multiscale damage analysis.

2. Material preparation and methods

2.1. Epoxy/carbon fiber composite

Cylindrical samples of carbon fiber-reinforced epoxy resin were initially prepared with different fiber angular orientations, as shown in Fig. 1. These included antisymmetric laminates of ±15°, +/30°, and a multilayer combination of ±15°/±30°/±45°/±86° To conduct thermochemical, physicochemical analyses and mechanical tests, rectangular samples measuring 130 mm in length, 20 mm in width and 3.3 mm in thickness were cut from the cylindrical samples using a rotational blade cutting machine.

2.2. Methods of characterization and experimental procedure

- **Microscopic observations:** A Scanning Electron Microscope (HITACHI 4800 SEM) was used to conduct microscopic observations and image analysis, with a particular focus on the composite microstructure, including fiber orientation and damage analysis in the cross-section.
- **Porosity measurement:** Porosity, or void fraction, represents the volume of void spaces in a material relative to its total volume. Pyrolysis is used to analyze the material's porosity. The fiber mass percentage (M_f%) and epoxy mass percentage (M_e%) were determined by subjecting all samples to pyrolysis at 550 °C for 5.5 h. This process led to the degradation of the matrix material, leaving only the carbon fiber. The fiber content was calculated using the following formula:

$$\text{Fiber content } (\%) = \left(\frac{M_0 - M_P}{M_0}\right) * 100$$

where M_0represents the initial mass and M_P represents the mass after pyrolysis. Furthermore, the densities of the carbon fiber (1.1 g/cm^3) and the epoxy resin (0.8 g/cm^3) were employed to ascertain the porosity content of the composite material.

- **Thermo-mechanical properties:** The main transition temperatures were initially measured using Differential Scanning Calorimetry (DSC), which was also employed to determine the specific heat capacity and analyze the curing behavior of the epoxy resins. The analysis was conducted using a DSC instrument (Q1000 V9.0 Build 275, TA Instruments). The samples were pressed into non-hermetic aluminum trays, sealed and heated to 220 °C at a rate of 10 °C/min, then cooled to 30 °C at the same rate.
- **Quasistatic tensile test:** Quasistatic tensile experiments were achieved using the Instron 5966 machine with a loading cell of 10 kN under a loading velocity of 10 mm/min and a temperature of 20 °C.
- **Fatigue test:** Tension-tension load-controlled fatigue tests have been conducted on the MTS 830 hydraulic fatigue machine at varying maximum loading levels (F_{max}). The minimum applied force (F_{min}) is always set at 10 % of the maximum applied force. The selected stress ratio is therefore (R_σ= 0.1), resulting in a mean loading level of 0.55 F_{max}. The experiments are conducted at a frequency of 10 Hz. To ensure accurate measurement of the reduction in stiffness due to the initial loading phase, each fatigue test is preceded by a quasi-static tensile loading-unloading-reloading phase. Tensile and fatigue tests were performed on the samples after a few rounds of polishing, with the geometry shown in Fig. 2.

2.3. Methodology of damage analysis in fatigue

To demonstrate the particular damage phenomena in CFRP composites, it is vital to create a benchmark for comparing different damage states and scenarios in various microstructures. This baseline provides a

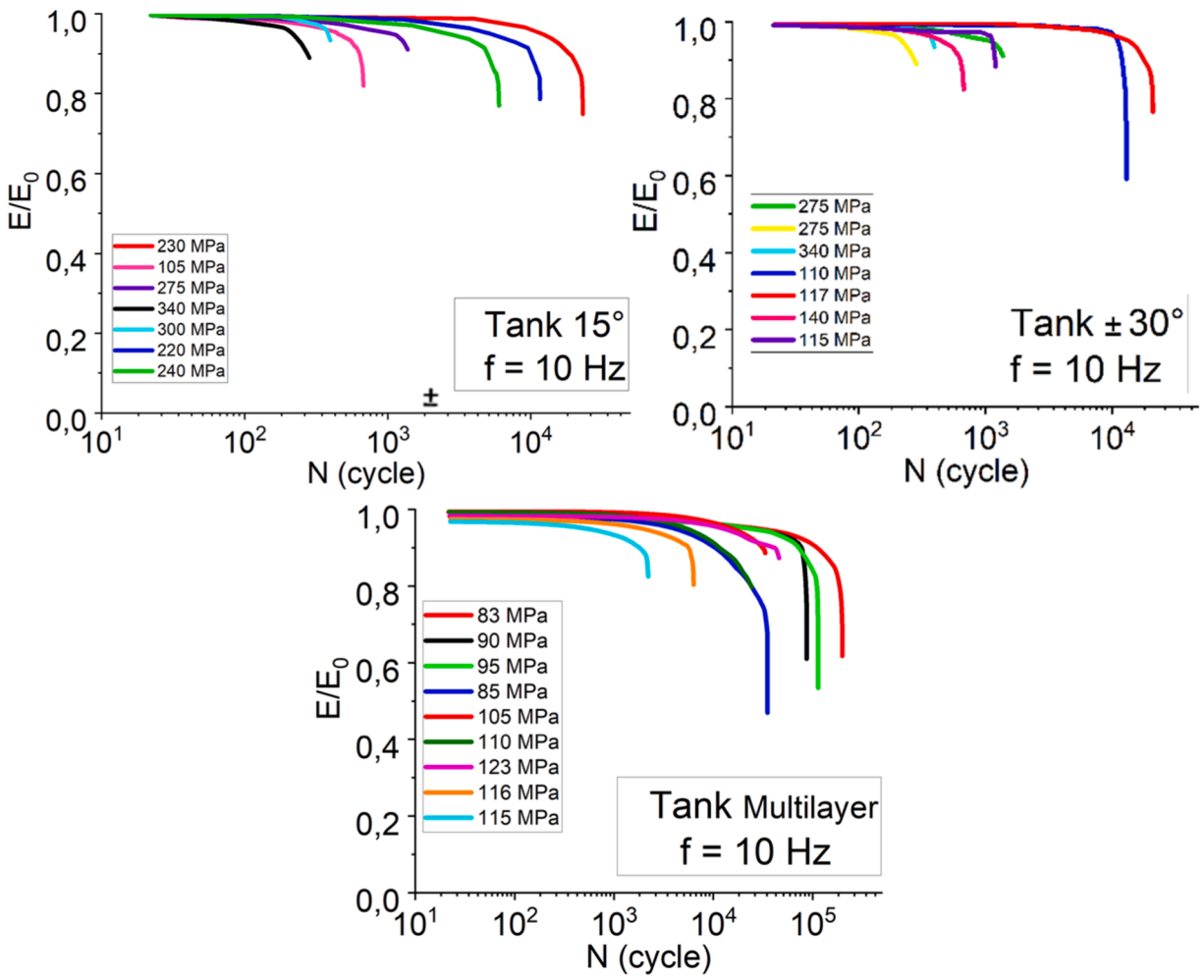

Fig. 8. Evolutions of the relative Young's modulus (E/E_0) during fatigue tests: (a) Tank ±15°, (b) Tank ±30° and (c) Tank Multilayer.

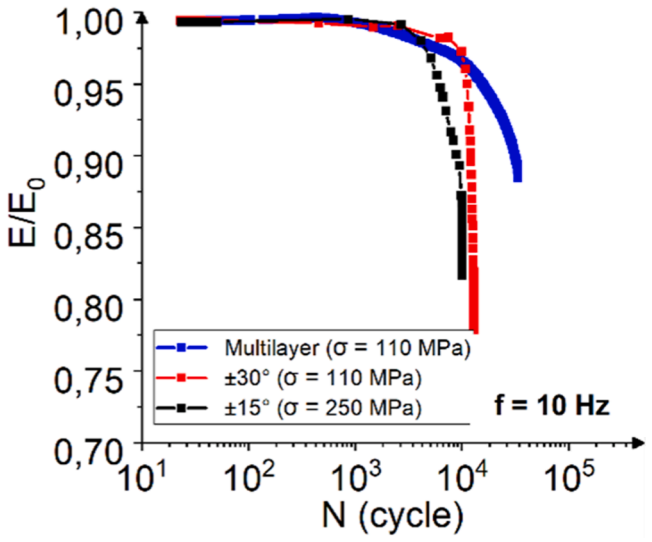

Fig. 9. Evolution of the relative Young's modulus (E/E_0) during fatigue tests.

comprehensive understanding of how damage affects the behavior of CFRP composites. Changes in stiffness are an important indicator of damage progression. Monitoring stiffness changes enables the tracking of microscopic damage mechanisms and residual stiffness across varying loading levels, providing a comprehensive and detailed overview of damage evolution.

The methodology involves conducting quasi-static loading and unloading tests, during which Young's modulus is quantified at each loading level. At each stage of the test, high-resolution SEM scans of the damaged areas are conducted to capture the microstructural changes and crack propagation. These detailed scans are essential for understanding the origin and progression of damage within the composite material. The process continues with repeated measurements and scans until the specimen fails. This approach allows for comprehensive monitoring of damage progression from initial crack formation to complete failure. By correlating the measured changes in Young's modulus with the observed microscopic damage mechanisms, it is possible to establish a quantitative relationship between macroscopic properties and the underlying damage phenomena. This relationship is of critical importance for understanding how different loading levels and microstructural configurations affect the overall integrity and functionality of carbon fiber-reinforced polymer (CFRP) composites. The value of this methodology lies in its ability to provide a clear and quantifiable link between damage at the microscopic level and the resulting changes in the material's mechanical properties. This information is crucial for the development of more durable and reliable composite materials, as it offers insights into damage mitigation and the enhancement of the material's resistance to failure. Fig. 3 illustrates the detailed methodology used to identify and understand the specific damage mechanisms in carbon fiber-reinforced polymer (CFRP) composites.

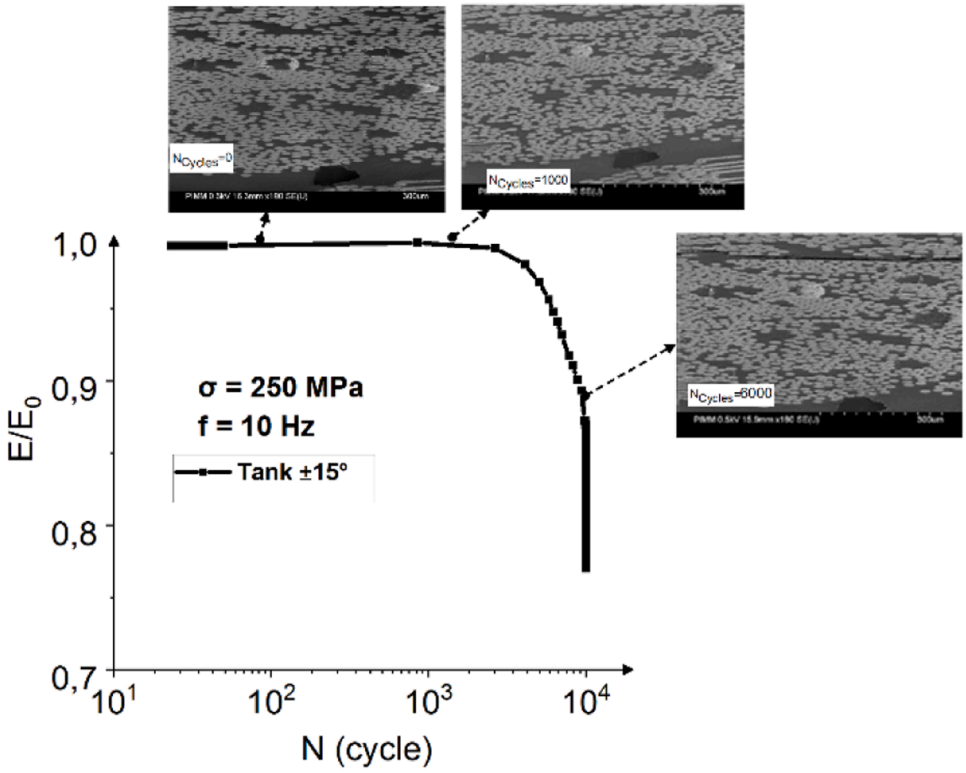

Fig. 10. Interrupted fatigue test coupled to microstructure observations for ±15°.

The figure provides a visual representation of the step-by-step process, beginning with the establishment of the baseline and concluding with the capture of SEM images and the analysis of the evolution of damage. This comprehensive approach ensures a comprehensive understanding of the intricate relationship between microstructural damage and macroscopic mechanical behavior in CFRP composites.

3. Experimental results and discussion

3.1. Microstructure analysis

The observations made under a scanning electron microscope (SEM) are presented in Fig. 4. The SEM micrographs confirm the structure of a laminated composite and validate the architecture manufactured by the industrial process. They also highlight the heterogeneity and state of the fiber/matrix interface. In each micrograph, porosities resulting from the manufacturing process can be observed, which may promote crack initiation.

3.2. Porosity measurement

Table 3 highlights the significant variations in porosity levels, ranging from 4.7 % to 7.8 %, in composite tubes with different fiber orientations. These findings emphasize the critical influence of fiber orientation on porosity within the composites. For the ±15° orientation, the composite density is 1.39 g/cm^3, with fibers accounting for 69.8% of the mass (54.2 % by volume) and epoxy for 30.2 % of the mass (38.0 % by volume), resulting in a porosity level of 7.8 %. In the ±30° orientation, the composite density is 1.45 g/cm^3, with fibers making up 70.9 % of the mass (57.3 % by volume) and epoxy 29.1 % of the mass (38.0 % by volume), leading to a porosity of 4.7 %. In the multilayer configuration, the density is 1.46 g/cm^3, with fibers constituting 72.9 % of the mass (59.2 % by volume) and epoxy resin 27.1 % of the mass (35.6 % by volume), with a porosity of 5.2 %. Overall, the average density across all tested tubes is 1.44 g/cm^3, with fibers representing 71.1 % of the mass (56.9 % by volume) and epoxy 28.8 % of the mass (37.5 % by volume). The average porosity for all samples is 5.4 %. These results underscore the importance of optimizing fiber orientation during the manufacturing process to minimize porosity, thereby improving the integrity and mechanical performance of the material (Table 1). .

3.3. Physico-chemical characterizations

Three orientations of carbon fiber-reinforced epoxy composites, namely ±15°, ±30°, and multilayers, were subjected to differential scanning calorimetry (DSC) to evaluate their thermal response to temperature variations. The DSC results for each orientation displayed a distinctive slope indicative of the phase change associated with the glass transition temperature (T_g), which was determined to be approximately 124 °C across all orientations tested. This indicates that the epoxy has been effectively cross-linked within the composite structure. Furthermore, no additional peaks or indications of physical aging were observed throughout the temperature range of 30 °C to 220 °C. This indicates that the composites maintained their thermal stability and did not undergo significant changes in molecular structure or thermal properties over the tested temperature range. In conclusion, the DSC analysis confirms that the carbon fiber reinforced epoxy composites with ±15°, ±30° orientations, and the multilayer configuration, have stable and well cross-linked resin matrices with consistent thermal behavior and resistance to physical ageing over the specified temperature range (Table 2).

3.4. Quasistatic tensile behavior

The mechanical properties of carbon fiber-reinforced epoxy composites, as illustrated in Fig. 5 and detailed in Table 3, exhibit significant variations influenced by fiber orientation. To ensure the reliability and repeatability of the stress-strain curves, approximately five specimens were analysed for each tested orientation ±15°, ±30°, and multilayer configurations. These results demonstrate the consistency of the tensile

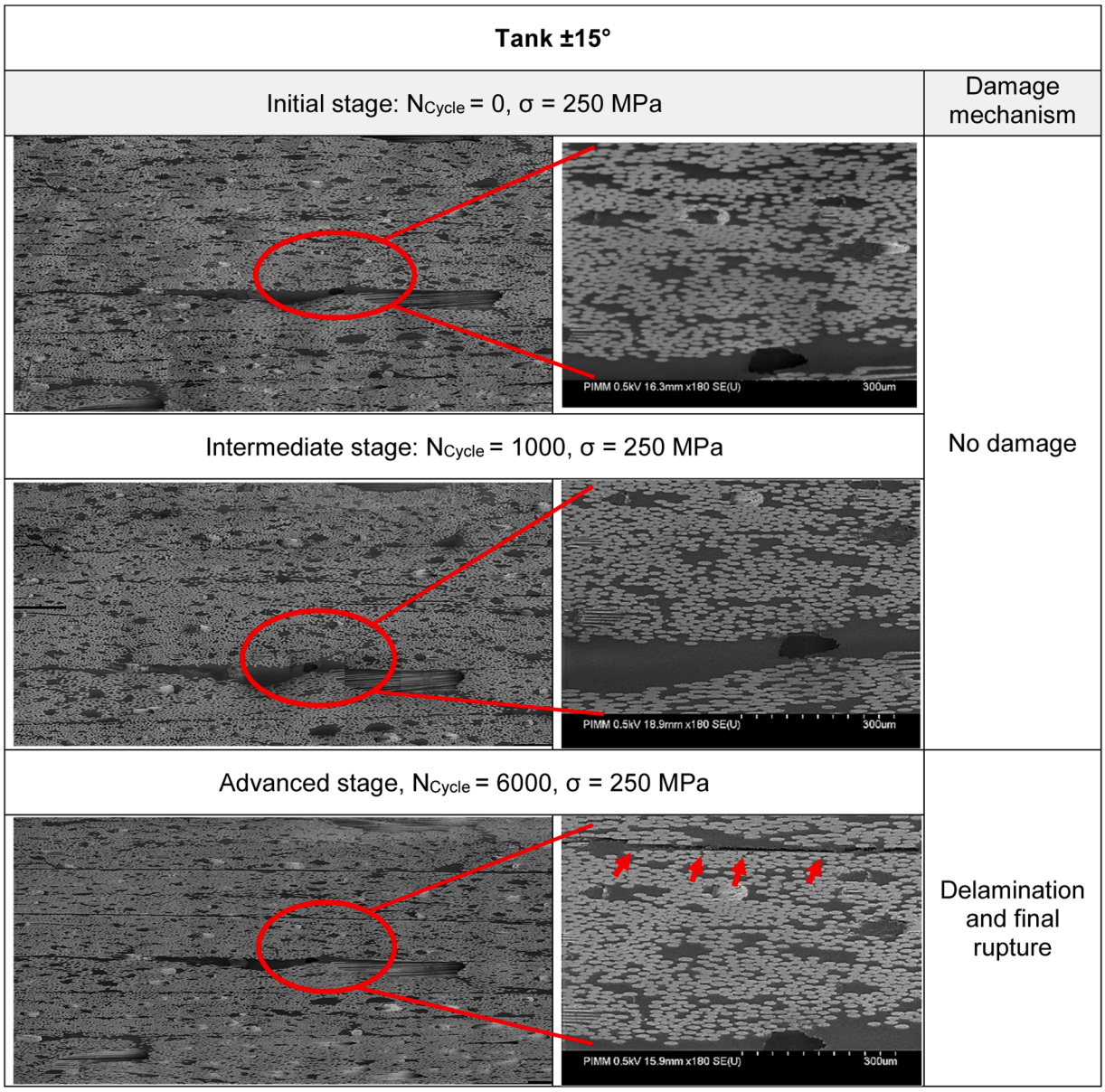

Fig. 11. Interrupted fatigue test and damage mechanisms: ±15°configuration.

behavior observed across multiple tests, providing a robust basis for further analysis. The results demonstrate that the orientation of the fibers has a significant impact on the mechanical behavior of carbon fiber-reinforced epoxy composites. Samples with fibers oriented in a direction parallel to the applied force, such as those in the ±15° orientation, exhibited higher tensile strength and modulus, indicating efficient load transfer along the fibers. Conversely, the ±30° and multilayer configurations exhibited greater ductility, as evidenced by their higher elongation at break.

The results demonstrate that the orientation of the fibers has a significant impact on the mechanical behavior of carbon fiber-reinforced epoxy composites. Samples with fibers oriented in a direction parallel to the applied force, such as those in the ±15° orientation, demonstrated enhanced tensile strength and modulus, indicating optimal load transfer along the fibers. In contrast, the ±30° and multilayer configurations demonstrate superior ductility, as evidenced by their higher elongation at break. In particular, the ±15° oriented samples exhibit superior performance due to optimal stress distribution along the fibers, resulting in higher stiffness and resistance to deformation. In contrast, the ±30° oriented specimens and multilayer configurations, where the fibers are less optimally aligned with respect to the loading direction, experience lower stiffness but demonstrate an enhanced ability to deform before failure. This behavior is attributed to damage and plastic deformation in the epoxy matrix, which reflects the influence of fiber-matrix interactions under load.

The transition from ductile to brittle fracture modes under varying loading conditions was investigated through microscopic analysis, as illustrated in Fig. 6. The micrographs of the specimens oriented at ±15° show features typical of brittle fracture, with flat, smooth, and featureless fracture surfaces. These lack the typical ductile characteristics observed in specimens oriented at ±30° The observed shift from brittle to ductile fracture modes as fiber orientation changes from ±15° to ±30° and multilayer configurations highlights the sensitivity of the material's fracture behavior to fiber orientation.

3.5. Fatigue behavior analysis: effect of the fiber orientation distribution

Fig. 7 shows the Wöhler curves derived from tension-tension fatigue

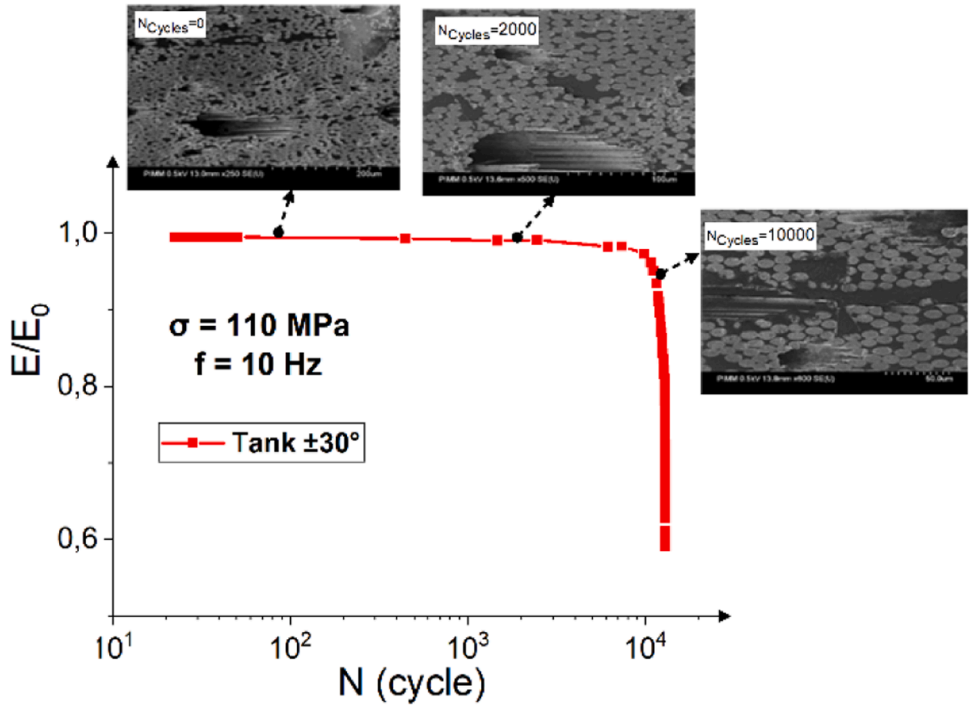

Fig. 12. Interrupted fatigue test coupled to microstructure observations for ±30°

tests at a frequency of 10 Hz for samples with fiber orientations of ±15°, ±30° and multi-layer configurations. These curves show the significant influence of the fiber orientation distribution on the fatigue behavior.

The ±15° configuration shows the superior fatigue resistance compared to the other configurations. Both the ±30° and Multilayer configurations show overlapping data points, indicating similar fatigue behavior.

The data show that an applied stress of approximately 120 MPa results in a fatigue life of approximately 10^3 cycles for the ±30° and mixed orientation samples. Conversely, an applied stress of approximately 90 MPa extends the fatigue life to approximately 10^5 cycles. This indicates that a 33 % reduction in applied stress can result in 100 times the fatigue life.

The results highlight the critical role of fiber orientation in determining fatigue life. In particular, fiber orientation can be optimized to improve the fatigue resistance of the material. For practical applications such as hydrogen tanks, this means that adjusting the fiber orientation can significantly improve the fatigue performance without significantly compromising the transverse properties of the material. In conclusion, the fatigue life of fiber reinforced composites is highly sensitive to the fiber orientation distribution. By strategically modifying the fiber orientation, it is possible to optimize the fatigue design and improve the durability of structures subjected to cyclic loading.

3.6. Multiscale analysis of fatigue damage

3.6.1. Macroscopic damage evolution

The damage mechanisms in specimens with different angular fiber orientations are shown in Fig. 8. The curves show the existence of different damage kinetics for different fiber orientations. Although the macroscopic damage patterns remain consistent for a given fiber orientation across different stress levels, the number of cycles to failure decreases as the stress amplitude increases. This observation is significant in the context of understanding the fatigue behavior of composites.

For all orientations tested, the curves show three distinct stages of damage evolution. The first stage is characterized by a linear constancy in damage. The second stage is characterized by a slow increase in damage. The third stage is characterized by a rapid increase in damage. A sharp decrease in stiffness finally leads to failure. These stages serve to elucidate the kinetics of damage progression, thereby enabling the refinement of micromechanical models for the purpose of predicting fatigue life and behavior in composite materials. Fig. 8 further illustrates the evolution of the relative modulus of elasticity (E/E_0) during tensile-tension fatigue testing at 10 Hz. In the case of high amplitude loading, the E/E_0 decreases rapidly in a linear logarithmic regime up to the point of failure. This process is accompanied by a significant amount of early damage within the laminate, particularly at the interfaces between different layers. These failures are predominantly interfacial in nature and manifest as delamination and fiber-matrix debonding. In contrast, the modulus decreases more gradually at lower amplitude loading. This is characterized by an initial rapid decrease due to early damage accumulation, a slower progressive decrease and a final sharp decrease prior to catastrophic failure. This gradual decrease is primarily controlled by matrix-fiber interactions, including matrix cracking.

The orientation of the fibers within the laminate has a significant effect on the fatigue behavior, with the ±15° orientation leading to a significant amount of early damage and a rapid decrease in modulus, whereas the ±30° and multi-layered orientations show a slower rate of degradation and a range of fracture behaviors (Fig. 9). It is therefore of great importance to gain an understanding of these evolutions if we are to develop and validate micromechanical models that will enable us to predict fatigue life and damage evolution in laminated composites. This knowledge will allow the optimization of laminate design by adjusting fiber orientations and improving interfacial properties, thereby improving the fatigue strength, mechanical performance, durability and reliability of composite structures in high load applications.

3.6.2. Microscopic damage evolution

To monitor the damage progression at the microstructural level during fatigue testing, interrupted fatigue tests were conducted in conjunction with microstructure observations for different angular orientations. Microscopic analysis was conducted on a 5 × 10 mm^2 observation zone, with each cycle examined individually as the number of cycles increased. Fig. 10 shows the outcomes for samples subjected to

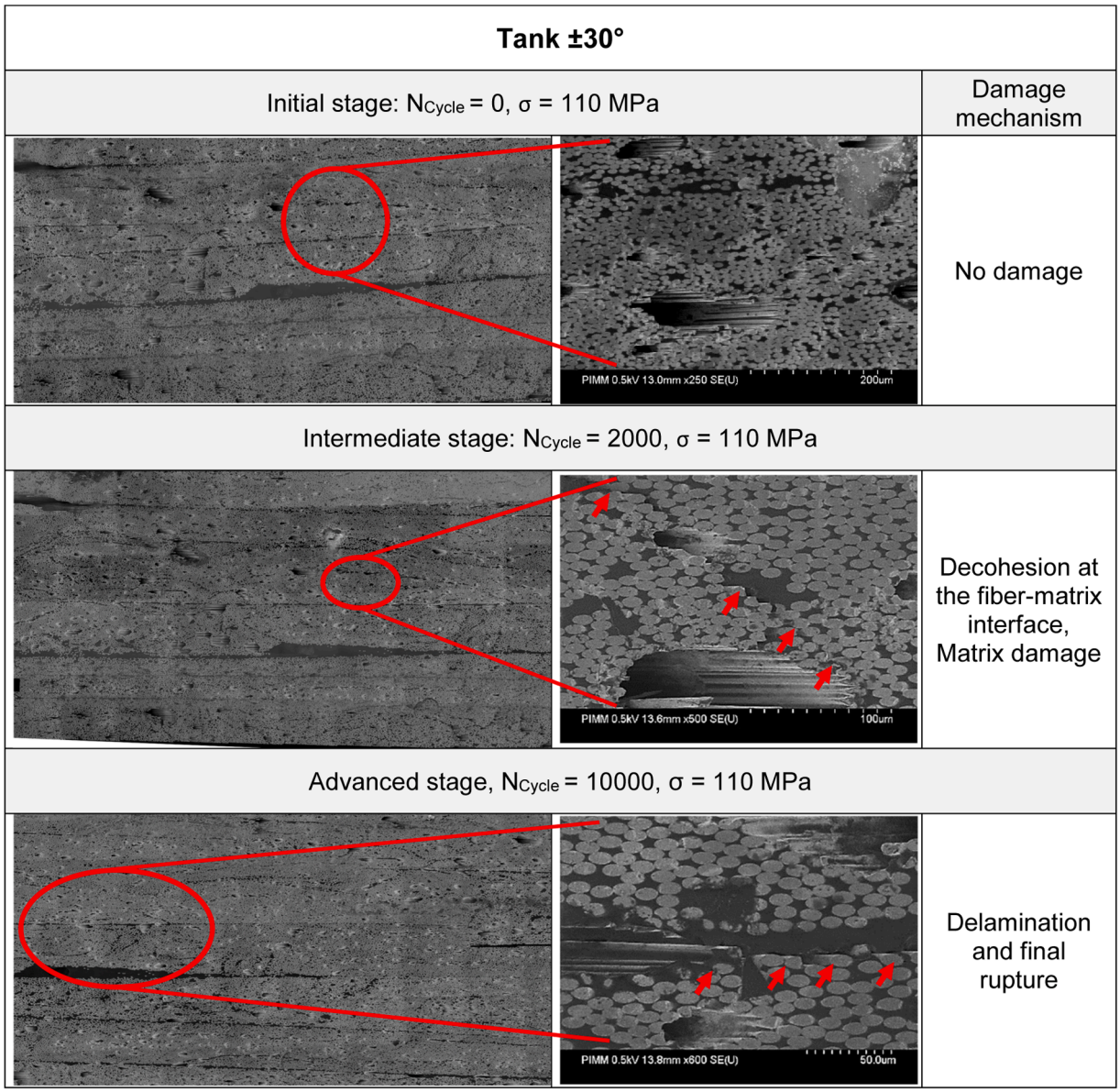

Fig. 13. Microscopic damage mechanisms: ±30 °configuration.

an applied stress amplitude of 250 MPa for the ±15° orientation at a frequency of 10 Hz.

Fig. 10 demonstrates the microscopic fatigue damage evolution of the ±15° oriented composite under loading. The ±15° configuration displays linear elastic behavior without any indication of damage up to 300 MPa (please refer to Fig. 5). Once this threshold is exceeded, damage accumulation begins, resulting in non-linear behavior and eventual failure. The initial stage is defined by a linear increase in damage. It is worth noting that the initial formation of damage, which manifested as matrix cracking and fiber-matrix debonding, was evident in samples oriented at ±15° This damage exhibited an early onset, particularly in these samples. As the number of cycles increased, damage to the matrix and at the fiber-matrix interface worsened, leading to delamination (see Fig. 11).

In the microstructures of ±15°, ±30°, and multilayer configurations, the composites initially exhibit the presence of pores or voids, which can be attributed to the manufacturing process. The aforementioned pores are randomly distributed throughout the material and frequently exhibit fibers extending to their surfaces. The heterogeneous distribution of fiber orientations across the layers gives rise to an uneven stress distribution during fatigue testing. The presence of pores in the material results in an amplification of fatigue stresses due to the disparity in stiffness between the matrix and the porous regions, which in turn gives rise to localized stress concentrations. As the applied loading increases, damage mechanisms propagate throughout the observation zone, originating at multiple pore locations. Concurrently, existing microcracks continue to expand. At the peak stress levels, a significant local deformation occurs via shearing around the fiber bundles, which results in pseudo-delamination near the fracture zones.

Figs. 12 and 13 present experimental fatigue tests coupled with microstructure observations for ±30° configuration, analyzed at different cycle stages: initial, intermediate, and final. In the initial stage, the material exhibits linear elastic behavior with no visible damage, as evidenced by the SEM image labeled "Initial stage" (Fig. 13).

The initial observed damage mechanism is decohesion at the fiber-matrix interface. As the number of cycles increases to approximately 2 $\times$ 10^3 cycles, damage continues to accumulate at a moderate rate. During this intermediate stage, the material exhibits signs of damage, as evidenced by the SEM image displaying the onset of decohesion at the fiber-matrix interface, micro-cracking, and subsequent matrix fracture.

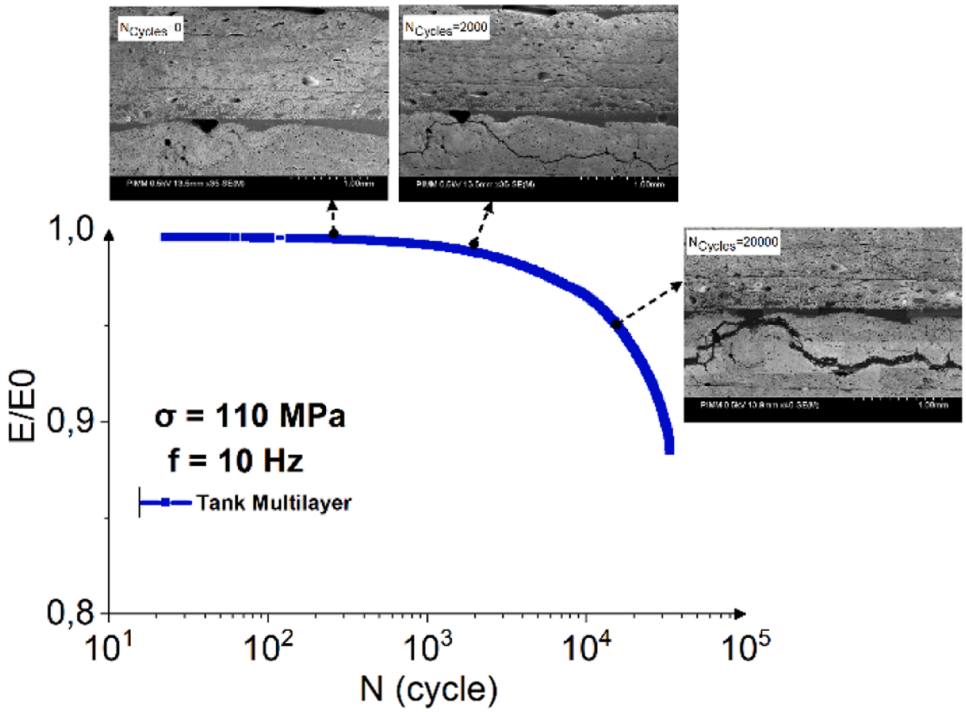

Fig. 14. Interrupted fatigue test coupled to microstructure observations for multilayer configuration.

The SEM image designated "Final Stage" (approximately 10^4 cycles) illustrates the presence of extensive cracks and significant damage, which ultimately leads to delamination and the complete failure of the material. The phenomena responsible for this damage include initial decohesion at the fiber-matrix interface, microcracking in the matrix, progression to matrix fracture, and development of large cracks resulting in delamination. This damage progression serves to highlight the critical stages of fatigue failure in fiber-reinforced composites and to underscore the importance of understanding these mechanisms for the purpose of improving material design and fatigue resistance.

Figs. 14 and 15 present the results for a multilayer configuration. The same damage scenario is observed for this composite configuration, namely that damage mechanisms propagate from multiple pore locations. It can be noted that damage propagation occurs at the $\pm 86^\circ$ layers of the multilayer composite (Fig. 15).

Indeed, the thresholds and kinetics of damage mechanisms in $\pm\theta$ composites are contingent upon a number of factors, including the specific orientation of fibers in each layer, the stress state experienced by each layer (which is influenced by the stacking sequence and macroscopic load), the statistical variation in pore spatial distribution (which varies with fiber orientation), and the rate at which load is applied. During fatigue testing, damage in long fiber composite structures manifests in a manner that varies according to the scale under consideration. At the microscopic level, the initiation of cracks within porosities plays a significant role in the damage of the material, including the separation of fibers and matrices at interfaces and the breaking of fibers, which in turn leads to the formation of new porosities.

It is crucial to understand the significance of these microscopic damage events in order to gain insight into the initial stages of composite failure. They serve to establish the conditions that facilitate further damage propagation, which is a key factor in the overall assessment of the material's resilience. At the mesoscopic scale, the coalescence of these microscopic decohesions results in the formation of transverse cracks that extend through the entire ply thickness (see Figs. 11, 13 and 15).

The ends of these transverse cracks become sites for microdelamination, which can further evolve into delamination between plies. It is therefore clear that this mesoscopic damage represents a critical factor in the overall structural integrity of the composite, as it directly impacts the load-bearing capacity and durability of the material. The complex interaction of multiple damage mechanisms in thick, heterogeneous composites requires the development of robust models to accurately predict their performance under load. It is essential that these models account for the various scales of damage, from microscopic crack initiation to mesoscopic crack propagation and delamination. It is crucial to gain insight into these interactions to enable the design of composites with enhanced durability and resistance to failure under cyclic loading conditions. To conclude, the specific fiber orientation, stress state, pore distribution and stress rate all have a significant impact on the damage mechanisms of $\pm\theta$ composites. At the microscopic level, the primary damage mechanisms are crack initiation within porosities and fiber/matrix decohesion. At the mesoscopic level, the coalescence of microscopic damage leads to transverse cracking and delamination. These findings highlight the importance of multiscale analysis in understanding and anticipating the behavior of carbon fiber-reinforced epoxy composites under cyclic loading.

3.7. *Fatigue fracture surface*

Fig. 16 presents the fractographic analysis of tube samples that have undergone fatigue testing. As previously outlined, the initial damage observed in these samples is the separation of fibers from the matrix. As the fatigue process continues, this can result in fiber breakage. The fractography of the multilayer carbon fiber epoxy composite reveals typical failure features, including fiber fracture, matrix cracking, fiber pull-out and potential delamination. These characteristics demonstrate the critical importance of fiber-matrix adhesion and the role of voids in the structural integrity of the composite material.

4. Conclusion

This study presents a comprehensive multi-scale analysis of fatigue and damage mechanisms in filament-wound carbon fiber-reinforced epoxy composites used for hydrogen storage tanks, with a particular

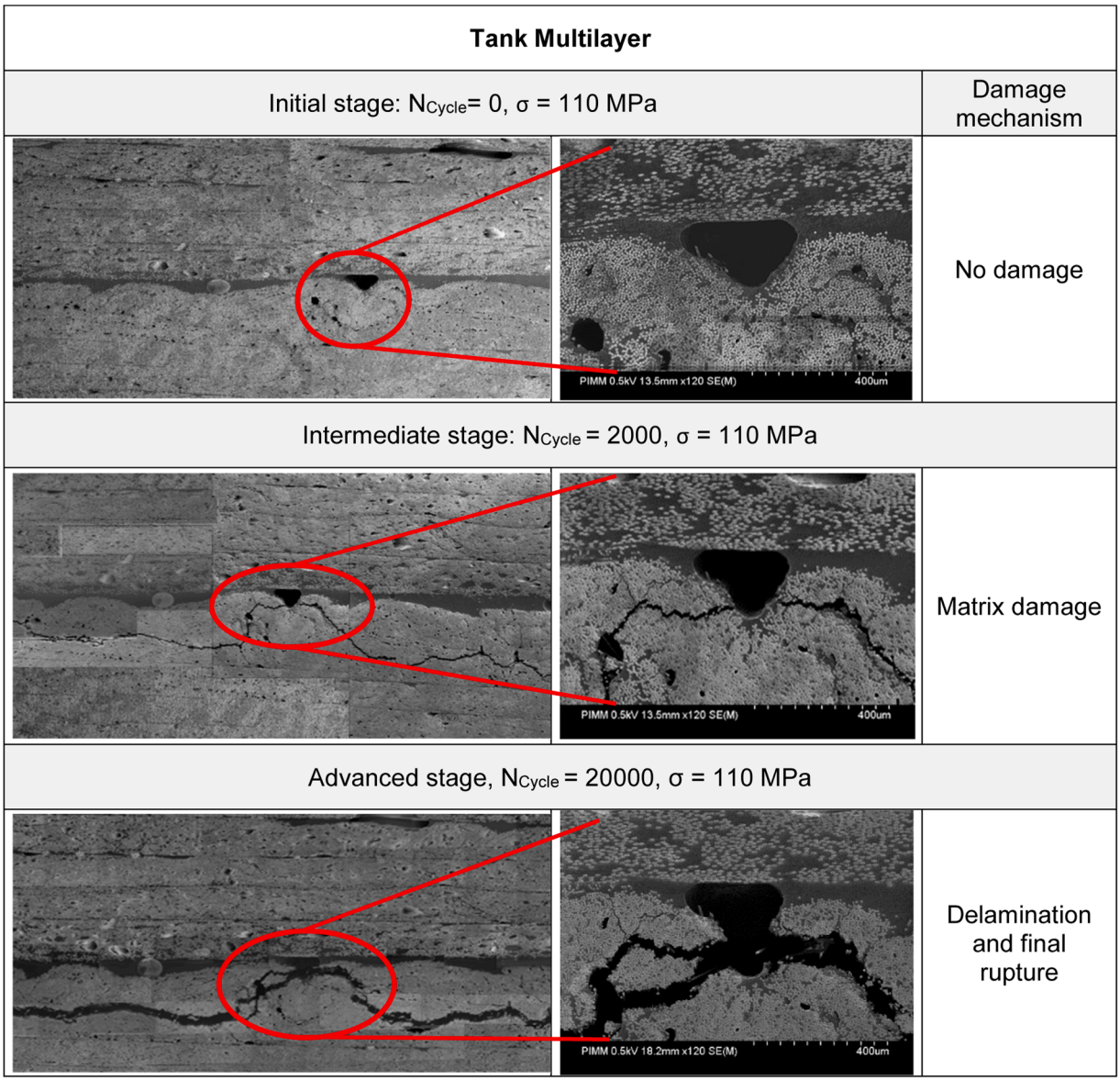

Fig. 15. Microscopic damage mechanisms: multilayers configuration.

focus on the effects of porosity. Three configurations were investigated: ±15°, ±30°, and multilayers. The results of the Differential Scanning Calorimetry (DSC) tests showed a stable thermal response across all orientations, with a consistent glass transition temperature (T_g) of around 124 °C. This confirms that the epoxy matrix has been effectively cross-linked, and that the material has demonstrated resistance to physical ageing.

The results of the quasi-static tensile tests demonstrated that the orientation of the fibers has a significant impact on the mechanical behavior. The ±15° configuration demonstrated superior tensile strength and modulus, ideal for load transfer, while the ±30° and multilayer configurations exhibited enhanced ductility. Microscopic analysis revealed a transition from brittle to ductile fracture modes with varying fiber orientations, emphasizing the role of fiber alignment in fracture behavior.

The analysis of fatigue behavior demonstrated the critical impact of fiber orientation on fatigue life. The ±15° configuration demonstrated superior fatigue resistance, while the ±30° and multilayer configurations exhibited fatigue performance that was similar to one another. The study demonstrated that a reduction in applied loading significantly extends fatigue life, emphasizing the importance of optimizing fiber orientation for enhanced fatigue performance in practical applications.

The macroscopic damage evolution was characterized by distinct stages: initial linear damage, slow progressive damage, and rapid damage leading to failure. The progression was influenced by fiber orientation, with different orientations exhibiting varying rates of damage accumulation. Microscopic analysis revealed that damage initiates at pores and evolves through matrix cracking and fiber-matrix debonding, leading to delamination and failure. The multiscale analysis revealed that damage mechanisms at the microscopic level, such as crack initiation and fiber/matrix decohesion, merge at the mesoscopic level to form transverse cracks and delamination. Gaining an understanding of these mechanisms is vital for accurately predicting the fatigue life and performance of composites. The study highlighted the need for robust models that account for multiscale damage interactions to improve composite design and durability under cyclic loading.

The fractographic analysis of fatigue-tested samples revealed typical failure features, including fiber fracture, matrix cracking, fiber pull-out and delamination. This highlights the critical importance of fiber-matrix adhesion and voids in the structural integrity of the composite material.

In conclusion, this research highlights the importance of fiber orientation, pore distribution and load state on the fatigue and damage

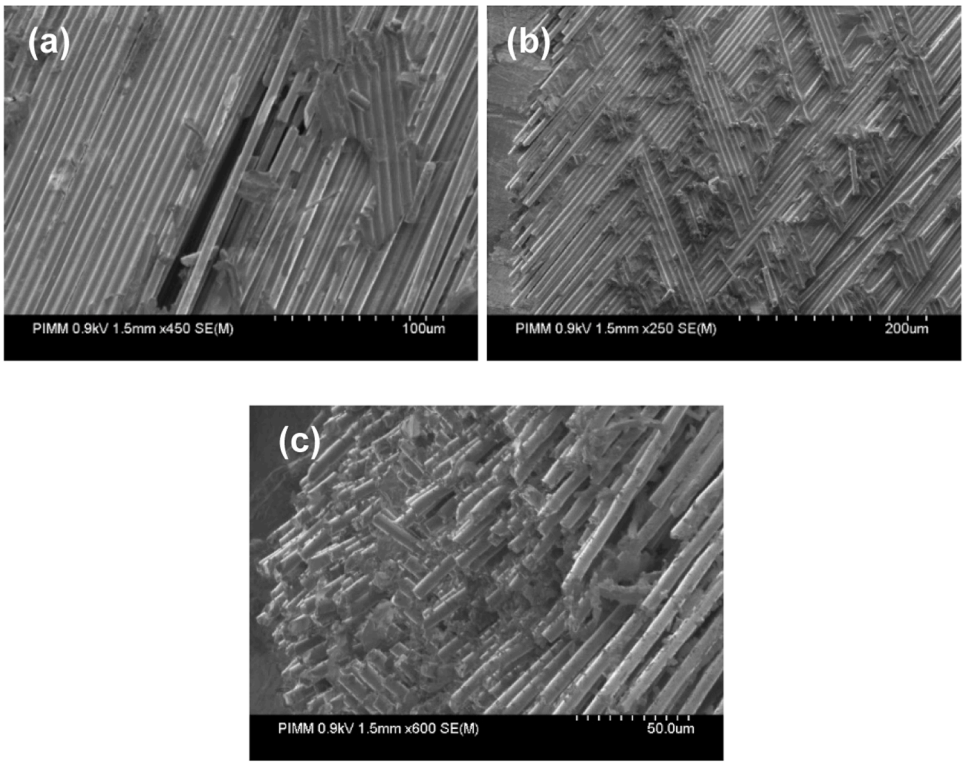

Fig. 16. Micrograph of fatigue fracture surface: (a)Tank ±15°, (b), Tank ±30° and (c) Tank Multilayer.

behavior of carbon fiber-reinforced epoxy composites. The findings provide valuable insights for optimizing the design and durability of hydrogen storage tanks and similar applications, demonstrating the efficacy of a multiscale approach in understanding and predicting composite performance under cyclic loading.

Consent to participate

Not applicable.

Consent to publish

Not applicable.

CRediT authorship contribution statement

Imen Feki: Writing – review & editing, Writing – original draft, Formal analysis. **Mohammadali Shirinbayan:** Writing – review & editing, Writing – original draft, Validation, Supervision, Project administration, Methodology, Formal analysis, Conceptualization. **Samia Nouira:** Writing – review & editing, Writing – original draft, Validation, Supervision, Methodology, Formal analysis. **Robert Tie Bi:** Writing – review & editing, Validation, Supervision, Project administration, Formal analysis, Conceptualization. **Jean-Baptiste Maeso:** Writing – review & editing, Validation, Supervision, Project administration, Methodology, Conceptualization. **Cedric Thomas:** Writing – review & editing, Validation, Supervision, Project administration, Conceptualization. **Joseph Fitoussi:** Writing – original draft, Validation, Supervision, Project administration, Methodology, Formal analysis, Conceptualization.

Declaration of competing interest

The authors declare that they have no conflicts of interest.

Data availability

The authors declare that the data and the materials of this study are available within the article.

References

[1] M.A.Ç. Cevahir Tarhan, A study on hydrogen, the clean energy of the future: hydrogen, J. Energy Storage (2021).
[2] A. H.T.H., Varma, Hydrogen storage for fuel cell vehicles, Curr. Opin. Chem. Eng. (2014).
[3] E. Rivard, M. Trudeau, K. Zaghib, Hydrogen storage for mobility: a review, Materials. (Basel) (2019).
[4] M. Melnichuk, G. Andreasen, H.L. Corso, A. Visintin, H.A. Peretti, Study and characterization of a metal hydride container, Int. J. Hydrogen Energy 33 (2008) 13.
[5] L.O. Spond, D.E. White, A storage tank for vehicular storage of liquid hydrogen, Appl. Energy (1980).
[6] G. Gondor, Pour le stockage de l'hydrogène : analyse thermodynamique de la formation d'hydrures métalliques et optimisation du remplissage d'un réservoir, HAL Id (2013) *tel-00782271*.
[7] K.H. Mori, Recent challenges of hydrogen storage technologies for fuel cell vehicles, Int. J. Hydrogen Energy (2009).
[8] H. Lara, Energy Revol. (2022). January 21,.
[9] L. Wang, C. Zheng, S. Wei, B. Wang, Z. Wei, Thermo-mechanical investigation of composite high-pressure hydrogen storage cylinders during fast filling, Int. J. Hydrogen Energy 40 (21) (2015) 6853–6859.
[10] M.C. Galassi, D. Baraldi, B.A. Iborra, P. Moretto, CFD analysis of fast filling scenarios for 70 MPa hydrogen type IV tanks, Int. J. Hydrogen Energy 37 (8) (2012) 6886–6892.
[11] H. Bie, X. Li, P. Liu, Y. Liu, P. Xu, Fatigue life evaluation of high-pressure hydrogen storage vessels, Int. J. Hydrogen Energy 35 (7) (2010) 2633–2636.
[12] J. Tomioka, K. Kiguchi, Y. Tamura, H. Mitsuishi, Influence of temperature on the fatigue strength of compressed-hydrogen tanks for vehicles, Int. J. Hydrogen Energy 36 (3) (2011) 2513–2519.
[13] L. Wang, C. Zheng, H. Luo, S. Wei, Z. Wei, Continuum damage modeling and progressive failure analysis of carbon fiber/epoxy composite pressure vessels, Compos. Struct. 134 (2015) 475–482.
[14] E.K. Gamstedt, R. Talreja, Fatigue damage mechanisms in unidirectional carbon-fibre-reinforced plastics, J. Mater. Sci. 34 (1999) 2535–2546.
[15] H. Dong, Z. Li, J. Wang, B.L. Karihaloo, A new fatigue failure theory for multidirectional fiber-reinforced composite laminates with arbitrary stacking sequence, Int. J. Fatigue 87 (2016) 294–300.

[16] L. Lasri, M. Nouari, M. El Mansori, Wear resistance and induced cutting damage of aeronautical FRP components obtained by machining, Wear. 271 (2011) 2542–2548.
[17] J. Fitoussi, M.H. Nikooharf, A. Kallel, M. Shirinbayan, Mechanical properties and damage behavior of polypropylene composite (GF50-PP) plate fabricated by thermocompression process under high strain rate loading at room and cryogenic temperatures, Appl. Compos. Mater. (Dordr) 29 (2022) 1959–1979.
[18] M. Shirinbayan, M. Rezaei-Khamseh, M.H. Nikooharf, A. Tcharkhtchi, J. Fitoussi, Multi-scale analysis of mechanical properties and damage behavior of polypropylene composite (GF50-PP) plate at room and cryogenic temperatures, Compos. Struct. 278 (2021) 114713.
[19] M.A. Imaddahen, M. Shirinbayan, H. Ayari, M. Foucard, A. Tcharkhtchi, J. Fitoussi, Multi-scale analysis of short glass fiber-reinforced polypropylene under monotonic and fatigue loading, Polym. Compos. 41 (11) (2020) 4649–4662.
[20] M. Shirinbayan, J. Fitoussi, N. Abbasnezhad, F. Meraghni, B. Surowiec, A. Tcharkhtchi, Mechanical characterization of a low-density sheet molding compound (LD-SMC): multi-scale damage analysis and strain rate effect, Compos. Part B: Eng. 131 (2017) 8–20.
[21] M. Shirinbayan, J. Fitoussi, M. Bocquet, F. Meraghni, B. Surowiec, A. Tcharkhtchi, Multi-scale experimental investigation of the viscous nature of damage in advanced sheet molding compound (A-SMC) submitted to high strain rates, Compos. Part B: Eng. 115 (2017) 3–17.
[22] M. Shirinbayan, J. Fitoussi, F. Meraghni, B. Surowiec, M. Bocquet, A. Tcharkhtchi, High strain rate visco-damageable behavior of advanced sheet molding compound (A-SMC) under tension, Compos. Part B: Eng. 82 (2015) 30–41.
[23] M. Shirinbayan, H.B. Rizi, N. Abbasnezhad, A. Tcharkhtchi, J. Fitoussi, Tension, compression, and shear behavior of advanced sheet molding compound (A-SMC): multi-scale damage analysis and strain rate effect, Compos. Part B: Eng. 225 (2021) 109287.
[24] H. Masaki, O. Shojiro, C.G. Gustafson, T. Keisuke, Effect of matrix resin on delamination fatigue crack growth in CFRP laminates, Eng. Fract. Mech. 49 (1994) 35–47.
[25] M. Shirinbayan, Multi-scale damage analysis of the tension-tension fatigue behavior of a low-density sheet molding compound (LD-SMC), J. Appl. Polym. Sci. (2021).
[26] M. Shirinbayan, J. Fitoussi, F. Meraghni, S. Farzaneh, B. Surowiec, A. Tcharkhtchi, Effect of a post-fatigue damage on the residual dynamic behavior of advanced-SMC composites, Appl. Compos. Mater. (Dordr) 26 (2019) 1313–1331.
[27] M. Shirinbayan, J. Fitoussi, F. Meraghni, M. Laribi, B. Surowiec, A. Tcharkhtchi, Coupled effect of loading frequency and amplitude on the fatigue behavior of advanced sheet molding compound (A-SMC), J. Reinf. Plast. Compos. 36 (4) (2017) 271–282.